Pergamon

*Int. J. Multiphase Flow* Vol. 23, No. 5, pp. 967–976, 1997

Printed in Great Britain
PII: S0301-9322(97)00016-5
0301-9322/97 $17.00 + 0.00

# DRAW RESONANCE OF OPTICAL MICROCAPILLARIES IN NON-ISOTHERMAL DRAWING

P. GOSPODINOV[1] and A. L. YARIN[2]†

[1]Institute of Mechanics, Bulgarian Academy of Sciences, Acad. G. Bonchev St. Bl. 4, Sofia 1113, Bulgaria
[2]Chemical Engineering Department and Rheology Research Center, University of Wisconsin–Madison, Madison, WI 53706-1691, U.S.A.

*(Received 14 March 1996; in revised form 18 February 1997)*

**Abstract**—The paper studies the process of drawing of glass microcapillaries from hollow cylindrical preforms, accounting for surface and gravity forces as well as for heat exchange with the surrounding medium. The quasi-one-dimensional model for hollow fiber drawing is generalized to include heat-transfer effects. The draw resonance (instability) phenomenon under non-isothermal conditions is studied and compared with the corresponding effect in the isothermal case. The method permits analysis of various flow regimes including stable steady-state drawing, sensitivity of fibers to external perturbations, drawing instability (self-sustained oscillations), and the effect of thermal conditions on the as-spun fibers. The frequency spectrum and correlation function of the time series corresponding to non-isothermal drawing are analyzed. The results show that under non-isothermal conditions (an additional degree of freedom) draw resonance continues to be a quasi-periodic phenomenon with no tendency to chaos. © 1997 Elsevier Science Ltd.

*Key Words:* hollow fiber spinning, draw resonance, non-isothermal effects

## 1. INTRODUCTION

Stability studies of isothermal drawing of filled (not hollow) fibers brought out the so- called draw resonance phenomenon, whereby the process loses its stability when the draw ratio $E = V_1/V_0$ exceeds the critical value of 20.22 (Pearson and Matovich 1969, Gelder 1971, Ishihara and Case 1975, Berman and Yarin 1983, Shultz and Davis 1984, and Yarin 1993). Effect of heat removal on draw resonance of filled fibers was studied in Shah and Pearson (1972a, b), Pearson and Shah (1973), Demay and Agassant (1982), and Yarin (1986, 1993). By contrast, drawing of hollow fibers (e.g. optical microcapillaries) earned less attention. The relevant theoretical studies date back to the works on thin sheets and tubular film flows in Taylor (1959) and Pearson and Petrie (1970a, b). Draw resonance threshold and arising self-sustained oscillations in isothermal regime of hollow fiber drawing were studied in Yarin *et al.* (1994), and the steady-state non-isothermal case was investigated in Yarin *et al.* (1989).

The theme of the present work is the effect of heat removal on draw resonance instability of hollow fiber drawing.

The drawing process is shown schematically in figure 1. A cylindrical glass tube with temperature $T_0$ is transported with a velocity $V_0$ to a furnace, where it is heated and softens. The dimensions of the tube are the median surface radius $R_0$ and wall thickness $h_0$, respectively. The tube is drawn with a velocity $V_1$ ($> V_0$) by a receiving device. As a result its radius shrinks to $R_1$ ($< R_0$). Outside the furnace the fiber is also cooled to a temperature $T_1$. The coordinate along the symmetry axis is denoted by $x$ and varies within the range $0 \leqslant x \leqslant L$, where $L$ is the characteristic draw length.

†On sabbatical leave from the Faculty of Mechanical Engineering, Technion—Israel Institute of Technology, Haifa 32000, Israel.

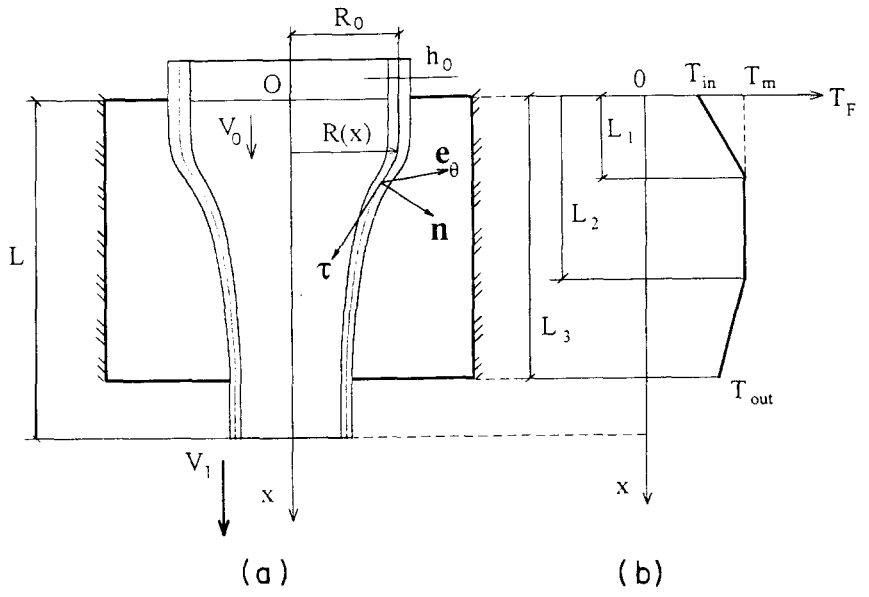


Figure 1. (a) Scheme of drawing process; (b) furnace wall temperature.

## 2. GOVERNING EQUATIONS

The quasi-one-dimensional continuity and momentum equations describing drawing of an axisymmetric hollow fiber were obtained in Yarin *et al.* (1994) using the integral balance method described in full detail in Yarin (1993). Then in van de Fliert *et al.* (1995) the systematic asymptotic expansion was used resulting in the same set of equations as those described in Yarin *et al.* (1994) (only the inertialess case was considered in van de Fliert *et al.* 1995). In Lee *et al.* (1996) oscillations of a hollow liquid shell were treated using the integral balance approach of Yarin *et al.* (1994). The integral balance approach of Yarin *et al.* (1994) is, in a sense, an asymptotic method employing the asymptotic expansion of velocity profile in fiber cross-section. Therefore, there is no wonder that the other asymptotic methods like that of van de Fliert *et al.* (1995) result in the same equations.

The equations described in Yarin *et al.* (1994) employ variables averaged over the fiber cross-section. Adopting the basic normal, azimuthal and tangent unit vectors $\mathbf{n}$, $\mathbf{e}_\theta$ and $\boldsymbol{\tau}$ associated with the generatrix of the median surface of the fiber wall, one arrives at the following set of equations (Yarin *et al.* 1994)

$$\frac{\partial}{\partial t}(Rh\lambda) + \frac{\partial}{\partial x}\left[Rh\left(V_\tau - \frac{1}{\lambda}\frac{\partial R}{\partial t}\frac{\partial R}{\partial x}\right)\right] = 0 \qquad [1]$$

$$\rho\left[Rh\lambda\frac{\partial V_\tau}{\partial t} + Rh\left(V_\tau - \frac{1}{\lambda}\frac{\partial R}{\partial t}\frac{\partial R}{\partial x}\right)\frac{\partial V_\tau}{\partial x} - \frac{Rh}{\lambda^2}\frac{\partial R}{\partial t}\frac{\partial^2 R}{\partial x \partial t} - hV_\tau kR\frac{\partial R}{\partial t} + \frac{Rhk}{\lambda}\left(\frac{\partial R}{\partial t}\right)^2\frac{\partial R}{\partial x}\right]$$

$$= \frac{\partial}{\partial x}(\Sigma_{\tau\tau}Rh) - \Sigma_{\theta\theta}h\frac{\partial R}{\partial x} + \rho gRh \qquad [2]$$

$$\rho\left[Rh\lambda\frac{\partial}{\partial t}\left(\frac{1}{\lambda}\frac{\partial R}{\partial t}\right) + Rh\left(V_\tau - \frac{1}{\lambda}\frac{\partial R}{\partial t}\frac{\partial R}{\partial x}\right)\cdot\frac{\partial}{\partial x}\left(\frac{1}{\lambda}\frac{\partial R}{\partial t}\right) + \frac{RhV_\tau}{\lambda}\frac{\partial^2 R}{\partial x \partial t} + hV_\tau^2\lambda kR - hV_\tau kR\frac{\partial R}{\partial t}\frac{\partial R}{\partial x}\right]$$

$$= \Sigma_{\tau\tau}h\lambda kR - \Sigma_{\theta\theta}h + 2\sigma(\lambda kR - 1) + (p_1 - p_2)R\lambda - \rho ghR\frac{\partial R}{\partial x}. \qquad [3]$$

The following notations are used: $R$ is the median surface radius ($R_0$ is its value in the hard preform); h is the wall thickness of the hollow fiber in direction normal to the median surface ($h_0$ is its value in the hard preform); $V_\tau$ is the liquid velocity along the generatrix of the median surface; $\rho$, $\sigma$, as well as $\mu$ and $c_p$ below are the density, surface tension, viscosity and heat capacity of the molten glass, respectively; $g$ is gravity acceleration; $t$ is time; $x$ is axial coordinate reckoned along the axis of the fiber; $\lambda$ is the arclength of an element of the generatrix; $k$ is the generatrix curvature; $p_1$ and $p_2$ are the gas pressures inside and outside the cavity of the hollow fiber. Here and hereinafter the subscripts $\tau$ and n denote vector projections on the longitudinal and normal directions, in particular, $V_\tau = \mathbf{V}\cdot\boldsymbol{\tau}$.

Equation [1] is the continuity equation, while [2] and [3] are, respectively, the projections of the momentum equation on the tangent and normal to the generatrix of the median surface. Longitudinal and azimuthal stresses in the fiber are given by the following expressions

$$\Sigma_{\tau\tau} = 2\mu\left\{\left[\frac{2}{\lambda}\frac{\partial V_\tau}{\partial x} + \left(\frac{1}{\lambda^2 R} - \frac{2k}{\lambda}\right)\right]\frac{\partial R}{\partial t} + V_\tau \frac{1}{\lambda R}\frac{\partial R}{\partial x}\right\} \quad [4]$$

$$\Sigma_{\theta\theta} = 2\mu\left[\frac{1}{\lambda}\frac{\partial V_\tau}{\partial x} + \left(\frac{2}{\lambda^2 R} - \frac{k}{\lambda}\right)\frac{\partial R}{\partial t} + V_\tau \frac{2}{\lambda R}\frac{\partial R}{\partial x}\right]. \quad [5]$$

Equations [1]–[5] are supplemented by the expressions for the arclength of the generatrix element $\lambda$ and the curvature of the generatrix $k$

$$\lambda = \sqrt{1 + \left(\frac{\partial R}{\partial x}\right)^2}, \quad k = \frac{1}{\lambda^3}\frac{\partial^2 R}{\partial x^2}. \quad [6]$$

To clarify the asymptotic nature of [1]–[5], we show here, for example, for the continuity equation [1] that an asymptotic approach (e.g. of Yarin 1983) beginning from the three-dimensional continuity equation yields the same result.

To find an asymptotic series for velocity profile in a cross-section of hollow film, we first consider radius-vectors of the free surfaces

$$\mathbf{r}_{\text{surf}}(t, x, \theta) = \mathbf{e}_x x + R(x, t)\mathbf{e}_r(\theta) \pm \frac{h(x, t)}{2}\mathbf{n}(t, x, \theta), \quad [7]$$

where $\mathbf{e}_x$ and $\mathbf{e}_r$ are, respectively, the unit vectors of the axial and radial directions.

Velocity at the free surface is defined as

$$\mathbf{v}_{\text{surf}} = \frac{\mathrm{d}\mathbf{r}_{\text{surf}}}{\mathrm{d}t} = \frac{\partial \mathbf{r}_{\text{surf}}}{\partial t} + \frac{\partial \mathbf{r}_{\text{surf}}}{\partial x}\frac{\mathrm{d}x}{\mathrm{d}t}, \quad [8]$$

where using [7] we find

$$\frac{\partial \mathbf{r}_{\text{surf}}}{\partial t} = R_{,t}\mathbf{e}_r \pm \frac{1}{2}(h_{,t}\mathbf{n} + h\mathbf{n}_{,t}) \quad [9]$$

$$\frac{\partial \mathbf{r}_{\text{surf}}}{\partial x} = \mathbf{e}_x + R_{,x}\mathbf{e}_r \pm \frac{1}{2}(h_{,x}\mathbf{n} + h\mathbf{n}_{,x}). \quad [10]$$

From geometrical considerations we obtain

$$\mathbf{n}_{,x} = -\lambda k\boldsymbol{\tau}, \quad \mathbf{n}_{,t} = -\lambda^{-2}R_{,xt}\boldsymbol{\tau}. \quad [11]$$

Consider also the liquid particle velocity at some point of the median surface $\mathbf{V}$ (absolute velocity), and the velocity of a point of the median surface with fixed longitudinal and azimuthal coordinates, $\mathbf{U}$. $\mathbf{U}$ is the velocity of the frame of reference associated with the median surface (reference-frame velocity). The absolute and reference-frame velocities are related as

$$\mathbf{V} = \mathbf{U} + \lambda\frac{\mathrm{d}x}{\mathrm{d}t}\boldsymbol{\tau} \quad [12]$$

which yields

$$\frac{dx}{dt} + \frac{V_\tau - U_\tau}{\lambda}. \tag{13}$$

Combining [7]–[11] and [13], we obtain

$$\mathbf{v}_{surf} = R_{,t}\mathbf{e}_r + \lambda^{-1}(V_\tau - U_\tau)\mathbf{e}_x + \lambda^{-1}(V_\tau - U_\tau)R_{,x}\mathbf{e}_r \pm \frac{1}{2}[h_{,t}\mathbf{n} - h\lambda^{-2}R_{,xt}\boldsymbol{\tau} + \lambda^{-1}(V_\tau - U_\tau)(h_{,x}\mathbf{n} - h\lambda k\boldsymbol{\tau})]. \tag{14}$$

The median surface of the film is given as $\mathbf{r} = \mathbf{R}^*(x, \theta, t) = \mathbf{e}_x x + R(x, t)\mathbf{e}_r(\theta)$.

Thus using [13] we obtain

$$\mathbf{V} = \frac{d\mathbf{R}^*}{dt} = R_{,t}\mathbf{e}_r + (\mathbf{e}_x + R_{,x}\mathbf{e}_r)\frac{dx}{dt} = R_{,t}\mathbf{e}_r + \lambda^{-1}(V_\tau - U_\tau)\mathbf{e}_x + \lambda^{-1}(V_\tau - U_\tau)R_{,x}\mathbf{e}_r. \tag{15}$$

Hence from [14] using [15] we arrive at the following non-dimensional expression

$$\mathbf{v}_{surf} = \mathbf{V} \pm \frac{\epsilon}{2}[h_{,t}\mathbf{n} - h\lambda^{-2}R_{,xt}\boldsymbol{\tau} + \lambda^{-1}(V_\tau - U_\tau)(h_{,x}\mathbf{n} - h\lambda k\boldsymbol{\tau})] \tag{16}$$

$$\epsilon = h_0/L \ll 1.$$

Here we use the following scales: $V_0$—for $\mathbf{v}_{surf}$, $\mathbf{V}$ and $\mathbf{U}$; $h_0$—for $h$ and the coordinate along the normal $y$ (see below); $L$—for $x$ and $R$; $L/V_0$—for $t$; $1/L$—for $k$, as well as for the nabla-operator $\nabla$ and $\mathbf{A}$ below.

Velocity profile $\mathbf{v}$ in a cross-section should be represented by the following asymptotic series

$$\mathbf{v} = \mathbf{V} + \epsilon\mathbf{A}y + \mathbf{O}(\epsilon^2). \tag{17}$$

At $y = \pm h/2$ it should yield [16], which allows to find $\mathbf{A}$ and to obtain $\mathbf{v}$ in the form

$$\mathbf{v} = \mathbf{V} + \epsilon\frac{y}{h}[h_{,t}\mathbf{n} - h\lambda^{-2}R_{,xt}\boldsymbol{\tau} + \lambda^{-1}(V_\tau - U_\tau)(h_{,x}\mathbf{n} - h\lambda k\boldsymbol{\tau})]. \tag{18}$$

The continuity equation, as usual, has the form

$$\nabla\cdot\mathbf{v} = \mathbf{0} \tag{19}$$

where according to Yarin *et al.* (1994), in the non-dimensional form

$$\nabla = \frac{1}{\epsilon}\mathbf{n}\frac{\partial}{\partial y} + \frac{\mathbf{e}_\theta}{R}\frac{\partial}{\partial\theta} + \frac{\boldsymbol{\tau}}{\lambda}\frac{\partial}{\partial x} + \mathbf{O}(\epsilon) \tag{20}$$

($\mathbf{e}_\theta$ is the unit vector of the azimuthal direction).

Substituting [18] in [19] and using [20] accounting for the first expression from [11] and the following geometric relations

$$\mathbf{n}_{,\theta} = \lambda^{-1}\mathbf{e}_\theta; \quad \boldsymbol{\tau}_{,\theta} = \lambda^{-1}R_{,x}\mathbf{e}_\theta; \quad \boldsymbol{\tau}_{,x} = \lambda k\mathbf{n}, \tag{21}$$

we arrive at the continuity equation for the leading order of magnitude

$$h^{-1}[h_{,t} + \lambda^{-1}(V_\tau - U_\tau)h_{,x}] + (\lambda R)^{-1}R_{,x}V_\tau + \lambda^{-1}V_{\tau,x} + (\lambda R)^{-1}V_n - kV_n = 0. \tag{22}$$

The normal velocity $V_n$ reads (Yarin *et al.* 1994)

$$V_n = \lambda^{-1}R_{,t}. \tag{23}$$

Accounting for the expression for $k$ in [6] and [23] we obtain

$$(\lambda R)^{-1}V_n - kV_n = (\lambda^2 R)^{-1}R_{,t}[1 - RR_{,xx}/(1 + R_{,x}^2)]. \tag{24}$$

Substituting [24] in [22] and multiplying by $Rh\lambda$, we obtain

$$R\lambda h_{,t} + RhV_{\tau,x} + R(V_\tau - U_\tau)h_{,x} + hR_{,x}V_\tau + \lambda^{-1}hR_{,t}[1 - RR_{,xx}/(1 + R_{,x}^2)] = 0. \tag{25}$$

We prove now that [25] is identical with the continuity equation [1] obtained by means of the integral balance method. Indeed, from [1] we obtain

$$h\lambda R_{,t} + R\lambda h_{,t} + Rh\lambda_{,t} + R_{,x}h(V_\tau - U_\tau) + Rh_{,x}(V_\tau - U_\tau) + Rh(V_{\tau,x} - U_{\tau,x}) = 0. \quad [26]$$

From the expression [6] for $\lambda$ we obtain

$$\lambda_{,t} = \lambda^{-1}R_{,x}R_{,xt}. \quad [27]$$

Since $\mathbf{U} = \partial\mathbf{R}^*/\partial t = R_{,t}\mathbf{e}_r$,

$$U_\tau = \lambda^{-1}R_{,t}R_{,x}. \quad [28]$$

Using [27] and [28] we obtain

$$Rh\lambda_{,t} - hR_{,x}U_\tau - RhU_{\tau,x} = -RhR_{,t}(\lambda^{-1}R_{,x})_{,x} - \lambda^{-1}hR_{,x}^2R_{,t} \quad [29]$$

and thus [26] reduces to

$$R\lambda h_{,t} + R_{,x}hV_\tau + R(V_\tau - U_\tau)h_{,x} + RhV_{\tau,x} + h\lambda R_{,t} - RhR_{,t}(\lambda^{-1}R_{,x})_{,x} - \lambda^{-1}hR_{,x}^2R_{,t} = 0. \quad [30]$$

Using the expression for $\lambda$ from [6], we rearrange the last three terms on the left in [29] to the form

$$h\lambda R_{,t} - RhR_{,t}(\lambda^{-1}R_{,x})_{,x} - \lambda^{-1}hR_{,x}^2R_{,t} = \lambda^{-1}hR_{,t}[1 - RR_{,xx}/(1 + R_{,x}^2)] \quad [31]$$

which shows that [30] is indeed identical with the asymptotic result [25]. Therefore, we indeed obtained the continuity equation [1] by means of the asymptotic expansion of the three-dimensional continuity equation [19].

The momentum equation might be obtained similarly.

As usual, the asymptotic approach is much more involved than the approach based on the integral balance method. The reason for this is the fact that three-dimensional differential equations of hydrodynamics have been obtained from the integral balance equations, and to arrive at the reduced quasi-one- (or two-) dimensional equations it is worth it to begin directly from the integral balance equations.

It is emphasized that the quasi-one-dimensional equations [1]–[5] are valid in the long wave approximation when $h/l \ll 1$ ($l$ being a characteristic scale in the longitudinal direction). This restriction does not imply that, in general, $kR \ll 1$ and $\partial R/\partial x \ll 1$ ($kR \approx 0$, $\lambda \approx 1$), since $R \gg h$. In the linear stability analysis of section 3 in Yarin *et al.* (1994) gently sloping hollow fibers were assumed, with $kR \ll 1$ and $\partial R/\partial x \ll 1$. However, in Yarin *et al.* (1994) it was also shown that these inequalities do not necessarily hold in fibers with finite perturbations, which are also considered in the present work. Therefore, we retain the corresponding terms in [1]–[3].

It should also be noted, that in Yarin *et al.* (1994) it was shown that small perturbations of isothermal, gently sloping filled and hollow fibers dominated by viscous force are governed by similar equations yielding identical instability thresholds. In the present work we treat large perturbations of non-isothermal hollow fibers in the situation when surface tension and gravity forces are of importance (as well as the inertial ones, to less extent), and the problem on hollow fibers cannot be reduced to that for the filled ones.

Note also that factors $(V_\tau - \lambda^{-1}R_{,t}R_{,x})$ on the left in [1]–[3], which are identical with $(V_\tau - U_\tau)$ according to [28] appear due to the fact that in a non-stationary case the frame of reference associated with the median surface moves with velocity $\mathbf{U}$ and thus the transfer of mass and momentum relative to a cross-section with a fixed value of $x$ occurs at a velocity $(\mathbf{V} - \mathbf{U})\cdot\boldsymbol{\tau} = V_\tau - U_\tau$. Similar factors appear in the theory of bending perturbations of filled free liquid jets moving in air with a high speed (Yarin 1993; Entov and Yarin 1984).

In non-isothermal flow, the viscosity of molten glass (the fiber-forming material) is a function of temperature, obeying the Arrhenius-type law (Doremus 1973)

$$\mu = \mu_0 \exp\left(\frac{A}{R_g T}\right), \quad [32]$$

where $\mu_0$ and $A$ denote the pre-exponential factor and the activation energy, $R_g$ is the universal gas constant and $T$ is the temperature. The latter is governed by the quasi-one-dimensional equation of energy balance

$$\rho c_p \left\{ \frac{\partial}{\partial t}(Rh\lambda T) + \frac{\partial}{\partial x}\left[ Rh\left( V_\tau - \frac{1}{\lambda}\frac{\partial R}{\partial t}\frac{\partial R}{\partial x} \right) T \right] \right\} = -(q_{n,1} + q_{n,2})\lambda R, \quad [33]$$

where heat conduction along the fiber is negligible relative to the heat exchange with the environment. The radiative heat flux in the outside normal direction is denoted by $q_{n,1}$, and its convective counterpart by $q_{n,2}$

$$q_{n,1} = \sigma_0 \epsilon [T^4 - T_F^4(x)] \quad [34]$$

$$q_{n,2} = \beta(x) \cdot [T - T_E(x)]. \quad [35]$$

The furnace wall temperature distribution is denoted by $T_F$, the effective gas temperature far from the fiber by $T_E$, $\epsilon$ is the emissivity of the fiber surface, $\beta$ is the convective heat transfer coefficient, $\sigma_0 = 5.68 \cdot 10^{-8}$ W/(m$^2$ °K$^4$) is the Stefan–Boltzmann constant.

Note that only heat exchange with the gas outside the fiber is accounted for, since heat losses into the fiber cavity are negligibly small.

The furnace wall temperature distribution is taken in the following form (see figure 1)

$$T_F(x) = \begin{cases} T_{in} + (T_m - T_{in}) \cdot x/L_1 & \text{for } 0 \leqslant x \leqslant L_1 \\ T_m & \text{for } L_1 \leqslant x \leqslant L_2 \\ T_m - (T_m - T_{out}) \dfrac{x - L_2}{L_3 - L_2} & \text{for } L_2 \leqslant x \leqslant L_3 \\ T_{E,out} & \text{for } L_3 \leqslant x \leqslant L, \end{cases}$$

where $T_{E,out}$ is the temperature of the gas environment outside the furnace, and $T_{in}$, $T_m$ and $T_{out}$ are the temperatures of the furnace wall at the inlet, middle and outlet of the furnace (see figure 1).

The effective temperature of the gas environment in the furnace is taken as the average of the fiber and furnace-wall temperatures

$$T_E(x) = \frac{T(x) + T_F(x)}{2}. \quad [37]$$

Given no external disturbances (dealing only with the stability problem), the constant input and output fiber velocities $V_0$ and $V_1$, as well as the initial median surface radius $R_0$, wall thickness $h_0$ and temperature $T_0$ are involved in the boundary conditions

$$V_\tau = V_0, \quad R = R_0, \quad h = h_0, \quad T = T_0 \quad \text{at} \quad x = 0$$

$$V_\tau = V_1, \quad \text{at} \quad x = L. \quad [38]$$

The steady-state solutions of Yarin *et al.* (1989) serve as the initial conditions for the stability problem

$$V_\tau = \varphi_1(x), \quad R = \varphi_2(x), \quad h = \varphi_3(x), \quad T = \varphi_4(x). \quad [39]$$

The problem posed above was normalized using the following scales: $L/V_1$ for $t$, $L$ for $x$, $R_0 E^{-1/2}$ for $R$ (draw ratio $E = V_1/V_0$), $h_0 E^{-1/2}$ for $h$, $V_1$ for $V_\tau$, $T_m$ for $T$. The following non-dimensional groups appear in the equations and initial and boundary conditions

$$\mathrm{Re} = \frac{\rho R_0 V_1}{\mu}\text{—Reynolds number}, \quad \mathrm{Fr} = \frac{V_1^2}{gR_0}\text{—Froude number},$$

$$\mathrm{Eu} = \frac{p_2 - p_1}{\rho V_1^2}\text{—Euler number},$$

$$\mathrm{We} = \frac{\rho V_1^2 R_0}{\sigma}\text{—Weber number,} \quad \mathrm{Bo} = \frac{\rho c_p V_1}{\sigma_0 T_m^3}\text{—Boltzmann number,}$$

$$E = V_1/V_0\text{—draw ratio,}$$

$$\pi_1 = \frac{A}{R_g T_m}, \quad \pi_2 = L/R_0, \quad \pi_3 = h_0/R_0.$$

In the non-isothermal case the value of $\mu_0$ is used instead of $\mu$ to calculate Re.

The heat-transfer parameter $\beta$ is calculated from the expression given by Ishihara and Kase (1975)

$$\beta(x) = \mathrm{Nu}\cdot R(x)^{-2/3}\cdot V_\tau(x)^{-1/3} \qquad [40]$$

($\beta$, $R$ and $V_\tau$ are non-dimensional) where the Nusselt number Nu is given by

$$\mathrm{Nu} = 1.983 \times 10^{-4}\pi^{-1/3}/(\rho c_p V_1^{2/3} R_0^{2/3}). \qquad [41]$$

Note that the numerical factor in [41] has a dimension $\mathrm{kg\cdot m^{1/3}/(s^{8/3}\cdot{}^\circ K)}$.

## 3. NUMERICAL IMPLEMENTATION, RESULTS AND DISCUSSION

A modified version of the algorithm developed in Yarin *et al.* (1994), and Gospodinov and Roussinov (1993a, b) was employed in the present work. The initial-value problem [1]–[3] and [33] was solved by a direct implicit scheme of the Crank–Nicholson type. Nonsymmetric approximations of the derivatives $R_{,x}$, $h_{,x}$, and $T_{,x}$, and symmetric ones for $V_{\tau,x}$, $V_{\tau,xx}$, and $R_{,xx}$ are used, with accuracy of the approximation $O(\Delta x^2)$. The time derivatives of $R$, $h$, $V_\tau$ and $T$ are approximated using a two-layer scheme with accuracy $O(\Delta t)$. Some more details on the numerical implementation might be found in Yarin *et al.* (1994).

The following values were used for the parameters in the simulations: $\rho = 3000\ \mathrm{kg/m^3}$, $\sigma = 0.25\ \mathrm{N/m}$, $c_p = 1000\ \mathrm{J/(kg\cdot{}^\circ K)}$, $V_1 = 0.05\ \mathrm{m/s}$, $R_0 = 0.005\ \mathrm{m}$, $h_0 = 0.001\ \mathrm{m}$, $L = 0.15\ \mathrm{m}$, and $\epsilon = 0.8$.

Two basic cases are considered here. The first is an isothermal process taking place under a constant temperature of approximately 1000°K (which is also the scale temperature $T_m$). The material viscosity is $\mu = \mu_0 = 10^5\ \mathrm{Pa\cdot s}$ and the corresponding Reynolds number $\mathrm{Re} = 7.5 \times 10^{-6}$. In this case there is no need to solve the energy equation. In the second, non-isothermal case the temperatures at the entrance and exit of the furnace, and that of the gas surrounding the fiber after it leaves the furnace, $T_{in}$, $T_{out}$ and $T_{E,out}$, are taken as 0.9 $T_m$ (with $T_m = 1000$°K), and $L_1/L = 0.3$, $L_2/L = 0.5$, and $L_3/L = 0.75$. The Reynolds number corresponding to the non-isothermal case was $\mathrm{Re} = 8.2 \times 10^{-3}$.

The following values were used for the non-dimensional groups in both cases: Fr = 0.051, $\mathrm{Eu} = 0.23 \times 10^2$, We = 0.15, $\mathrm{Bo} = 2.64 \times 10^3$, $\pi_1 = 6$, $\pi_2 = 30$, $\pi_3 = 0.2$, and $\mathrm{Nu} = 8.375 \times 10^{-8}$. Under the given conditions the steady-state value of the radius of the as-spun fiber is $R(1, 0) = 0.964$, since for Eu > 0 outside pressure is larger than the inside one.

Self-sustained oscillations (a fully developed draw resonance) of the radius of the as-spun hollow fiber emerging at the supercritical draw ratio of 400 after the draw resonance sets in are shown in figure 2. It is seen that in the non-isothermal case the effect of cooling manifests itself in reduction of the period and amplitude of the oscillations. A similar trend was found in non-isothermal drawing of filled fibers in Yarin (1986, 1993) where self-sustained oscillations were of smaller amplitude in the non-isothermal case when draw ratio was the same as in a corresponding isothermal one. To resolve the nature of arising self-sustained oscillations corresponding to fully developed draw resonance (after the transient is over) the spectral power density $P$ and the correlation function $F$ were studied:

$$P(\omega) = \frac{\mathrm{d}}{\mathrm{d}\omega}\left[\frac{1}{2\Phi}\int_{-\Phi}^{\Phi} R^2(1, t)\mathrm{d}t\right] = \frac{|R_\Phi(\omega)|^2}{2\pi\Phi} \qquad [42]$$

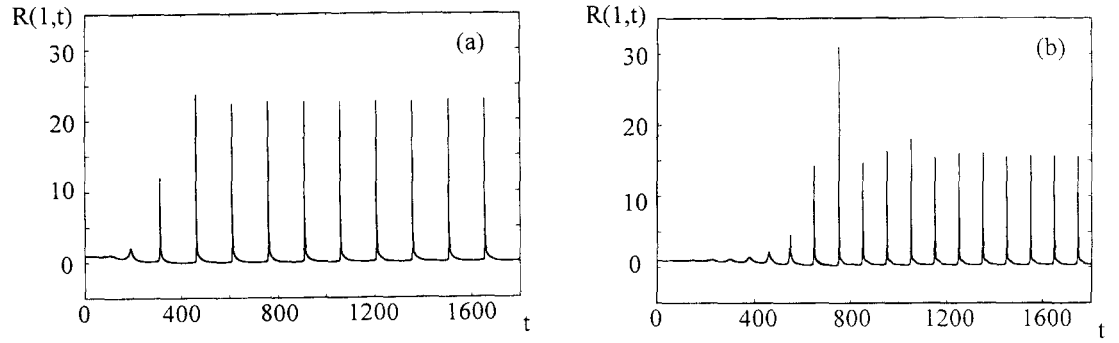


Figure 2. Development of self-sustained oscillations in isothermal and non-isothermal cases; $E = 400$. (a) isothermal case; (b) non-isothermal case.

with

$$R_\Phi = \int_{-\Phi}^{\Phi} R(1, t)\mathrm{e}^{-i\omega t}\,\mathrm{d}t$$

$$F(\tau) = \frac{1}{\Phi}\int_0^{\Phi} R(1, t)R(t + \tau)\mathrm{d}t \qquad [43]$$

as the period $\Phi$ tends to infinity.

In the numerical implementation $R_\Phi$ was found using a standard FFT-algorithm. $|R_\Phi|^2 = R_\Phi \cdot R_\Phi^*$, where the star superscript denotes the complex conjugate.

The spectral power corresponding to figure 2(a) and (b), is shown in figure 3(a) and (b), respectively. It brings out the multimodal quasiperiodic character of the highly nonlinear oscillations in fully developed draw resonance. The frequency corresponding to the highest spectral peak is $\omega = 0.0414$ and $\omega = 0.0568$ in the isothermal and non-isothermal cases, respectively.

The correlation functions corresponding to the isothermal and non-isothermal cases of figure 2 are plotted in figure 4. In evaluating it, the period $\Phi$ was taken as 300. In both cases the correlation function approaches a periodic behavior, as is foreseen for periodic time series. Variation of the governing parameters did not result in a tendency to any chaotic behavior of the oscillations. A similar situation was found before for the filled-fiber drawing in Yarin (1986, 1993).

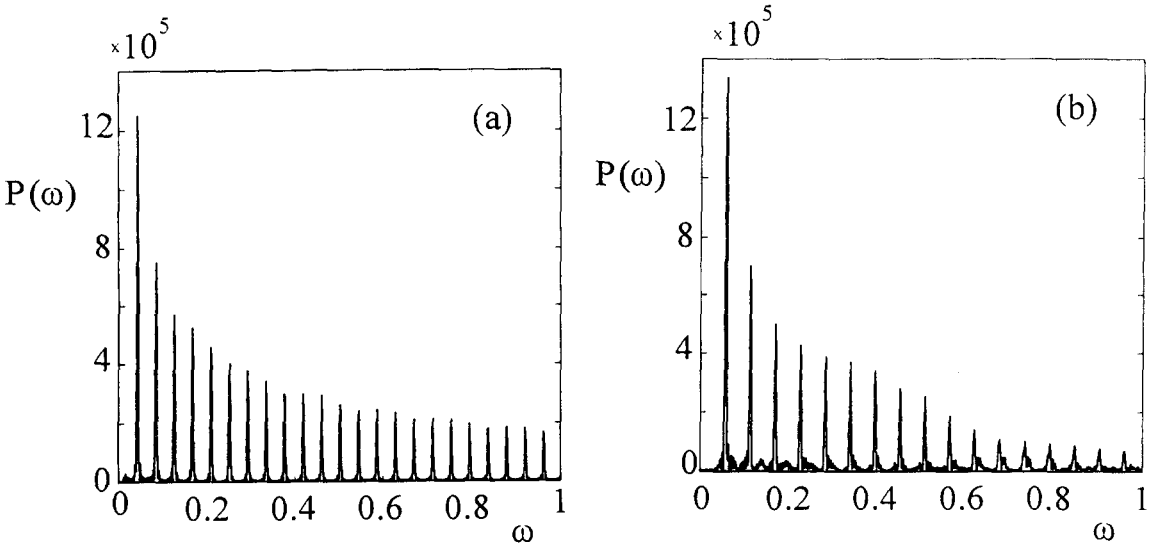


Figure 3. Distribution of the spectral power density corresponding to figure 2(a) and (b), respectively.

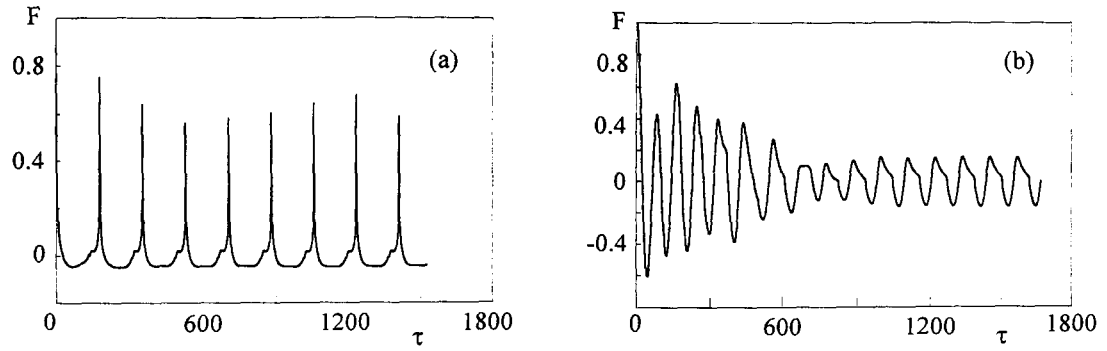


Figure 4. Correlation functions corresponding to figure 2. (a) Isothermal case; (b) non-isothermal case.

The temperature of the as-spun hollow fiber at the receiving device oscillates under the non-isothermal draw resonance regime as per figure 5. The temperature time series is also quasiperiodic.

## 4. CONCLUSION

The approach developed in the present work allows one to predict the behavior of a spinline in the case of non-isothermal drawing of hollow fibers (optical microcapillaries). The effect of fiber cooling on the characteristics of the draw resonance is studied. The method can be also employed for prediction of the effect of external excitation on the characteristics of as-spun hollow fibers.

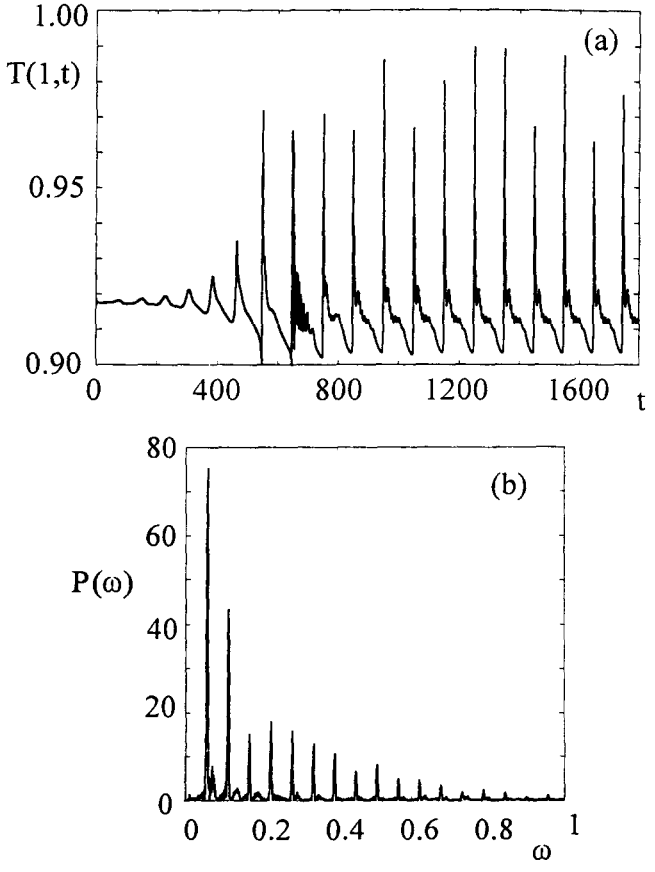


Figure 5. Non-isothermal case: (a) fiber temperature oscillations at the receiving device ($x = 1$); (b) distribution of the spectral power density corresponding to the temperature time series.

Cooling reduces period and amplitude of self-sustained oscillations arising due to draw resonance as compared to the isothermal case. The latter is similar to that found previously for the filled fiber drawing.

Analysis of the spectral power density and the correlation function corresponding to radius and temperature variation of as-spun hollow fibers shows that self-sustained oscillations continue to be quasiperiodic. No tendency to chaos was found in spite of the fact that a new degree of freedom (temperature variation) was involved.

*Acknowledgements*—This work was partially supported by the Bulgarian National Foundation, Grant number TN 577/95.

## REFERENCES

Berman, V. S. and Yarin, A. L. (1983) Dynamical regimes of fiber spinning. *Fluid Dyn.* **18,** 856–862.

Demay, Y. and Agassant, J. F. (1982) Application de la stabilité linéaire à l'étude du filage textile isotherme et non isotherme. *J. Méc. Théor. et Appl.* **1,** 763–772.

Doremus, R. H. (1973) *Glass Science*. Wiley, New York.

Entov, V. M. and Yarin, A. L. (1984) The dynamics of thin liquid jets in air. *J. Fluid Mech.* **140,** 91–111.

Gelder, D. (1971) The stability of fiber drawing processes. *Ind. Eng. Chem. Fund.* **10,** 534–535.

Gospodinov, P. and Roussinov, Vl. (1993a) Drawing of optical fibers under nonsteady heat exchange. *Mech. Res. Comm.* **20,** 129–135.

Gospodinov, P. and Roussinov, Vl. (1993b) Nonlinear instability during the isothermal draw of optical fibers. *Int. J. Multiphase Flow* **19,** 1153–1158.

Ishihara, H. and Kase, S. (1975) Studies of melt spinning. V. Draw resonance as a limit cycle. *J. Appl. Polym. Sci.* **19,** 557–565.

Lee, C. P., Anilkumar, A. V. and Wang T. G. (1996) A theoretical model for centering of a thin viscous liquid shell in free and forced capillary oscillations. *Phys. Fluids* **8,** 2580–2589.

Pearson, J. R. A. and Matovich, M. (1969) Spinning a molten threadline. Stability. *Ind. Eng. Chem. Fund.* **8,** 605–609.

Pearson, J. R. A. and Petrie, C. J. S. (1970a) The flow of a tubular film. Part 1. Formal mathematical representation. *J. Fluid Mech.* **40,** 1–19.

Pearson, J. R. A. and Petrie, C. J. S. (1970b) The flow of a tubular film. Part 2. Interpretation of the model and discussion of solutions. *J. Fluid Mech.* **42,** 609–625.

Pearson, J. R. A. and Shah, Y. T. (1973) Stability analysis of the fiber spinning process. *Trans. Soc. Rheol.* **16,** 519–533.

Schultz, W. W. and Davis, S. H. (1984) Effects of boundary condition on the stability of slender viscous fibers. *J. Appl. Mech.* **51,** 1–5.

Shah, Y. T. and Pearson, J. R. A. (1972a) On the stability of nonisothermal fibre spinning. *Ind. Eng. Chem. Fundam.* **11,** 145–149.

Shah, Y. T. and Pearson, J. R. A. (1972b) On the stability of nonisothermal fibre spinning—general case. *Ind. Eng. Chem. Fundam.* **11,** 150–153.

Taylor, G. (1959) The dynamics of thin sheets of fluid. I. Water bells. *Proc. R. Soc. London* **A253,** 289–295.

van de Fliert, B. W., Howell, P. D. and Ockenden, J. R. (1995) Pressure-driven flow of a thin viscous sheet. *J. Fluid Mech.* **292,** 359–376.

Yarin, A. L. (1983) On the dynamical equations for liquid jets. *Fluid Dyn.* **18,** 134–136.

Yarin, A. L. (1986) Effect of heat removal on nonsteady regimes of fiber formation. *J. Eng. Phys.* **50,** 569–575.

Yarin, A. L. (1993) *Free Liquid Jets and Films: Hydrodynamics and Rheology*. Longman, Harlow and Wiley, New York.

Yarin, A. L., Gospodinov, P. and Roussinov, Vl. (1994) Stability loss and sensitivity in hollow fiber drawing. *Phys. Fluids* **6,** 1454–1463.

Yarin, A., Roussinov, V., Gospodinov, P. and Radev, P. (1989) Quasi-one-dimensional model of drawing of glass microcapillaries and approximate solutions. *Theor. Appl. Mech.* **20,** 55–62.